Transition from Moderate to Strong Hydrogen Bonds: Its Identification and Physical Bases in the Case of O−H···O Intramolecular Hydrogen Bonds

Yitbarek H. Mariam* and Ryza N. Musin

Department of Chemistry and Center for Theoretical Studies of Physical Systems, Clark Atlanta University, Atlanta, Georgia 30314

Received: August 19, 2007; In Final Form: September 24, 2007

A systematic investigation aimed at identifying the transition from moderate (M) to strong (S) hydrogen bonds (HBs) and the physical bases of the main geometry-based HB strength classifications reported in the literature has been undertaken using the quantum theory of atoms in molecules (QTAIM). Correlations between the Laplacian of the electron density (ρ) at the O···H hydrogen bond critical points (HBCPs), $\nabla^2\rho_{hb}$, specifically between the more intuitive parameter $L_{hb} = -\nabla^2\rho_{hb}$ and other QTAIM parameters, have also been explored. The transition from MHBs to SHBs has been identified as the minimum (maximum) in the geometric dependence of L_{hb} ($\nabla^2\rho_{hb}$). For O−H···O intramolecular (IM) HBs (including resonance-assisted HBs), the transition is obtained, in a truly remarkable agreement with the existing geometry-based HB strength classifications, when the O···O (O···H) distance is ∼2.51 (∼1.55) Å and when the ratio of the potential energy density ($|V_{hb}|$) to the kinetic energy density (G_{hb}) ≈ 1.3. Accordingly, the ranges of the $|V_{hb}|/G_{hb}$ ratios are >2−1.3 and 1.3−1 for, respectively, SHBs and MHBs. When the O···O distance is not a genuine indicator of HB strength, the $|V_{hb}|/G_{hb}$ ratio and other parameters should be considered to characterize the strength of the HBs. Rationalizations have been provided by way of decoding the physical bases of the transition in terms of the properties of ρ and the mechanical characteristics of the interactions that created the HBCPs. L_{hb} was found to correlate, with a very high degree of fidelity, with at least three parameters (in addition to O···O and O···H distances and the IMHB energy), V_{hb}/G_{hb}, H_{hb}/ρ_{hb} (the ratio of the total energy density, H_{hb}, to the electron density, ρ_{hb} (the so-called bond degree parameter)), and δ_{hb}(O,H) (the delocalization index), demonstrating the importance and utility of L_{hb} ($\nabla^2\rho_{hb}$) for the study of HB interactions. A new refined energetics-based classification of O−H···O IMHB strengths has been advanced. The approach taken in this investigation can be extended to other HB systems.

Introduction

Numerous reports, reviews, monographs, and books, dating back to the early 1920s,[1] have been published[2] on the different roles the hydrogen bonds (HBs) play in various areas of the sciences including DNA and protein structures and functions, reactivity, and crystal engineering. The role that strong HBs have been presumed to play in biochemical reaction mechanisms and enzyme catalyses has also been pursued with some fascination.[3] The strengths (spanning up to 50 or more kcal/mol)[4,5] and classifications of HB interactions have been the foci in most of the studies on HBs. Accordingly, three main classifications based on energetic (EC),[6] geometrical (GC),[7] and physicochemical (PCC)[8] criteria have been advanced. Because these classifications are of pertinence to this report, it is useful to highlight their essential features.

Different EC-based classifications have been proposed over the years as can be seen in the summary below.[4] Needless to say, given that the basis for the classifications is solely the energetics of the interactions, it would be desirable to reconcile them into one single scheme. This has not been done as of yet because the internal border between moderate and strong HBs has not been established. According to one of the key features of the PCC classification,[8] strong O−H···O HBs exist when the O···O distance, D(O···O), is shorter than 2.5 Å, and a further decrease in D(O···O) is accompanied by a lengthening of the O−H bond and by a shortening of the O···H bond until a symmetrical HB may be reached for D(O···O) ≈ 2.39−2.40 Å.

classification basis	weak	moderate/strong	strong/very strong
energetic (kcal/mol)	1−4	4−15	15−40
			15−60
energetic (kcal/mol)	<5	5−10	>10
energetic (kcal/mol)	2−12	12−24	>24

The GC-based classification, which is particularly pertinent to this report, is the first comprehensive classification of homonuclear O−H···O HBs,[7] which was advanced by Gilli and co-workers (referred to as GBFG hereafter) on the basis of a large set of neutron and X-ray crystal-structure evidence. The classification consists of three major categories with D(O···O) (in Å) used to delimit the HB strengths: (A) three classes of very strong HBs consisting of negative-charge-assisted HBs ((−)CAHBs; 2.3−2.5), positive-charge-assisted HBs ((+)CAHBs; 2.36−2.43), and resonance-assisted strong HBs (RAHBs; 2.39−2.55; for all RAHBs the range is 2.39−2.7); (B) one class of moderate HBs, i.e., polarization-assisted HBs (PAHBs; 2.65 to ≥2.75); (C) one overall class of weak, isolated HBs (IHBs; 2.7 to ≥2.85). GBFG have also advanced the electrostatic−covalent HB (ECHB) model, according to which weak HBs are electro-

* Author to whom correspondence should be addressed. Phone: (404) 880-6846. Fax: (404) 289-2085. E-mail: ymariam@cau.edu.

10.1021/jp076668i CCC: $40.75
Published on Web 12/08/2007

static in nature but become increasing covalent with increasing HB strength.[9]

Notwithstanding the types of classifications summarized above, Desiraju recently advanced the hydrogen-bond-without-internal-border (HBWIB) concept/model.[10] According to this HBWIB model, the HB is a borderless interaction and is envisioned as being electrostatic, with variations toward covalency among the so-called very strong HBs, and toward van der Waals character in the domain of the weak HB.[10] Both the ECHB[9] and the HBWIB[10] models are inherently consistent with the origins of hydrogen bonding as delineated by Morokuma decomposition analysis.[11] The HBWIB concept is not, thus, fundamentally different from the ECHB model except that it presumes that the transition from weak to medium strong to strong HBs is too difficult to determine. Parthasarathi et al.[5] have recently used the quantum theory of atoms in molecules (QTAIM) approach[12] both to understand the HBWIB concept and to quantify the transition from weak to moderate to strong hydrogen bonding. But their conclusions suggested that they, if not tacitly, at least implicitly embraced the HBWIB concept.[5] Does this mean then that the various classifications, which were based on empirical observations, have outlived their utility and importance? The present study seeks, in part, to reconcile such competing views by establishing what the physical bases of particularly the PCC-[8] and GC-based[5] classifications might be.

QTAIM remains one of the methods of choice for the study of HB interactions because it can provide quantitative measures for the interactions. Accordingly, "closed-shell" and "shared" interaction limits can be considered using the local virial equation (eq 1)[12,13]

$$(\hbar^2/4m)\nabla^2\rho(r_c) = V(r_c) + 2G(r_c) \quad (1)$$

where $\nabla^2\rho(r_c)$ is the Laplacian of the electron density (ρ), $G(r_c)$ (always positive) is the electronic kinetic energy density, and $V(r_c)$ (always negative[12]) is the electronic potential energy density (all evaluated at bond critical points). To put $V(r_c)$ and $G(r_c)$ on equal footing, the relation for the total energy density, $H(r_c)$, has been defined as eq 2[14]

$$H(r_c) = V(r_c) + G(r_c) \quad (2)$$

In the context of the above relations, shared-shell (SS) interactions are dominated by lowering the potential energy $V(r)$ and are obtained when $\nabla^2\rho(r_c) \leq 0$ (or when $2G(r_c) + V(r_c) \leq 0$; in this region $H(r_c) < 0$). In contrast, "purely closed-shell" (PCS)[15] interactions are obtained when both $H(r_c) > 0$ and $\nabla^2\rho(r_c) > 0$. The intermediate region between these two limits is the closed-shell (CS); i.e., interactions with $H(r_c) < 0$ and $\nabla^2\rho(r_c) > 0$ and may be characterized as partially covalent.[14,16,17]

Numerous reports had used QTAIM for the study of HB interactions.[15−29] For the sake of brevity, we make specific reference here only to two of the reports that are most pertinent to this report. On the basis of the ratio $|V(r_c)|/G(r_c)$, Espinosa et al.[15] recently proposed a classification of HB strengths. According to this classification, PCS interactions are obtained when $|V(r_c)|/G(r_c) < 1$, SS interactions when $|V(r_c)|/G(r_c) > 2$, and CS interactions when $|V(r_c)|/G(r_c)$ is between 1 and 2. Espinosa et al.[15] have also advanced the ratio $H(r_c)/\rho(r_c)$ as a bond degree parameter to assess the covalent nature of the interactions. More recently, Grabowski et al.[29] used a combination of the QTAIM approach and variation−perturbation partitioning of the intermolecular interaction energy to characterize the covalent nature of HB interactions. In that study, they established that the ratio of the delocalization and electrostatic terms of ~0.45 constituted the approximate borderline between covalent and noncovalent HBs. In both of these studies and in all other QTAIM-based studies, the internal border between moderate (M) HBs (MHBs) and strong (S) HBs (SHBs) was not identified.

One may argue that the delimitations in the GC-based classification[7] are not unique HB internal borders, because the physical bases for the GC classification have not been delineated yet. In fact, despite the GC-based classification being based on D(O···O) distances,[7] physical insights that may be extracted from a systematic study of the dependence of QTAIM parameters on D(O···O) remain unexplored. It therefore seems reasonable to investigate such dependence so that the physical bases for the GC classifications may be found. The primary goal of this work is therefore to establish the transition from MHBs to SHBs so that the link among the different classifications can be established thereby paving the way to reformulate HB classifications that use the same internal borders as references for demarcation. The Laplacian ($\nabla^2\rho$) can provide a wealth of chemical information in this regard because it is a sensitive probe for identifying spatial changes of charge concentration not evident in the electron density ρ itself.[26,27] However, the dependence of $\nabla^2\rho$ on D(O···O) and the link between $\nabla^2\rho$ and other QTAIM parameters have not been investigated systematically when it comes to HB interactions. A second goal of this work is, therefore, to establish the nature of such links. Furthermore, a third goal of the research is to extend our QTAIM one-electron property studies to two-electron properties, more specifically, pair-density indices (PDIs).[30] By providing authoritative support for the physical bases of the MBHs-to-SHBs transition, the report will demonstrate that the classifications of HB strengths deduced from empirical observations were actually truly remarkable. The investigation will also establish several cases of intercorrelations between $\nabla^2\rho$ and other QTAIM parameters as well as advance a refined or more complete energetics-based classification of O−H···O IMHB strengths.

Theoretical Overview and Computational Details

Theoretical Overview. The concepts and terminology of QTAIM have been reviewed elsewhere,[12,27] and for the sake of brevity no review will be presented in this report. Reviews on the concepts of electron delocalization (within QTAIM[31,32]) and various reports on its applications are also available,[33] and hence only an overview will be presented here. Within Hartree−Fock theory, the delocalization index (DI), δ(A,B), is defined as[30,34,35]

$$\delta(\mathrm{A,B}) = 4\sum_i \sum_j S_{ij}(\mathrm{A})S_{ij}(\mathrm{B}) \quad (3)$$

where S_{ij}(A) and S_{ij}(B) denote the overlap of a pair of spatial orbitals over atoms or functional groups A or B. DIs have contributions of both spins in a closed-shell system. Also, both AB and BA contributions have to be included. Hence, these contributions are accounted for by the factor in eq 3.[30] DIs are interpreted as the number of electron pairs delocalized or shared between atoms A and B. δ(A,B) has a finite value whether atoms A and B are or are not bonded. In the former case, i.e., if bonded (or if atoms A and B share an interatomic surface and a bond path), δ(A,B) is used to count the number of electron pairs shared between the bonded atoms;[36] furthermore, when no significant charge transfer exists between atoms A and B, δ(A,B) can be interpreted as a bond order or index.[30]

Computational Details. For consistency purposes with an earlier report from our group[37] and because the B3LYP method[38]

CHART 1: Systems Investigated

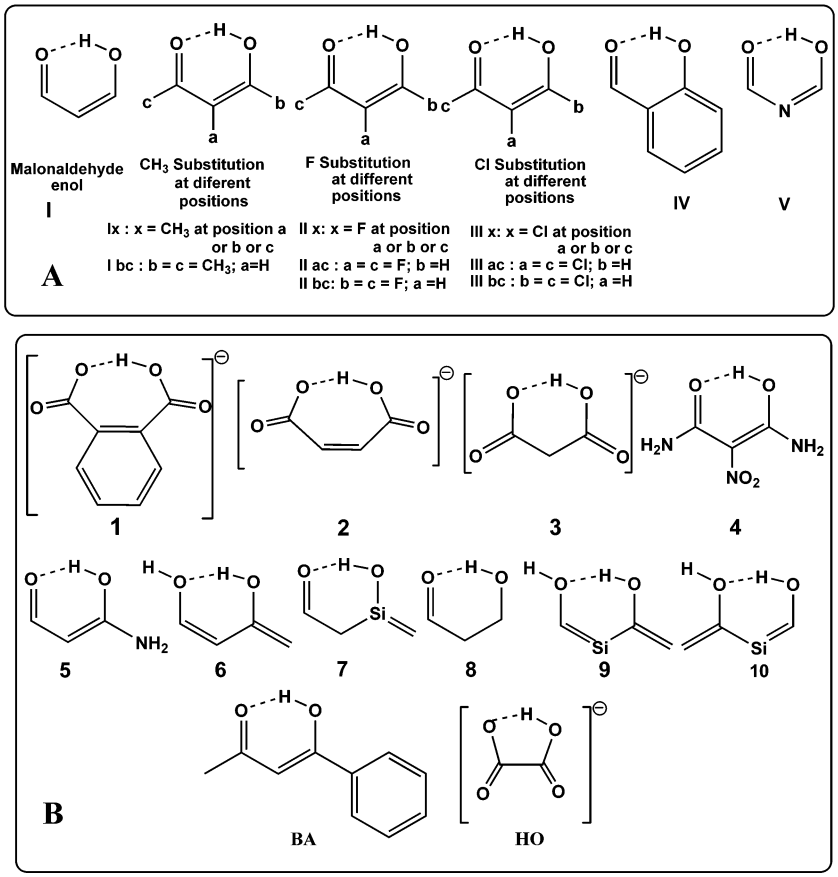

has been shown to give good results for the types of systems investigated in the present work,[39] the B3LYP/6-311++G(d,p) model was used for the quantum chemical calculations. Calculations at the MP2/6-311++G(d,p) level have also been done on a majority of the systems both as benchmark calculations and for electron-pair-density analysis.[12] (Details on the model chemistry have been provided in our previous communication.[37]) Default options of the Gaussian 98 or Gaussian 03W[40] suite of programs were used unless specified otherwise. The Spartan program[41] was also used at both the B3LYP and the MP2 or resolution image MP2 (RIMP2) levels along with the 6-311++G-(d,p) basis set. In all cases, frequency (harmonic) calculations have been performed to ensure that the structures are equilibrium geometries. Atoms in molecules topological analyses were carried out in accordance with Bader's approach[12] using AIM2000.[42] The DENSITY = CURRENT option was used to generate the wavefunction files (for topological analyses).

Electron-pair-density, $\rho(r,r')$, analyses were done at the HF/6-311++G(d,p)//MP2/6-311++G(d,p) level because the AIM2000 program[42] that we have used is not suited to calculate DIs from wavefunctions obtained at the B3LYP and MP2 levels. It has been pointed out that because Coulomb correlation reduces electron pairing HF results of DI calculations present upper limits for the values.[30,35,43] However, DIs calculated using Kohn−Sham orbitals have been found to be slightly larger than those obtained using HF orbitals.[44] The DI calculations were limited to atom pairs forming the IMHB, and for such pairs the DIs obtained cannot be interpreted as bond indices because of unequal sharing of electrons between the atoms. Hence, because we are interested in establishing the connection between DIs and other QTAIM parameters and not in bond indices, we have chosen the use of HF theory for this work as a reasonable compromise. Such a choice has been made by others based on similar rationale.[30] In all of the DI calculations, the relative and absolute accuracies of the integration steps were set to 10^{-5}. The radii of spheres for radial integration for H and O were set at, respectively, 0.3 and 0.5. The integrated Laplacian, $L(\Omega)$, was checked to assess the numerical accuracy of atomic integrations. $L(\Omega)$ was $\leq 1 \times 10^{-5}$ for H and $\leq 1 \times 10^{-3}$ for O, which were deemed acceptable.

Systems Investigated. The systems investigated include intramolecular O−H···O HBs consisting a wide spectrum of HB strengths ((−)CAHBs, RAHBs, and weak HBs (WHBs)). Shown in Chart 1A are CH_3−, F−, and Cl− derivatives of malonaldehyde and systems **IV** and **V**, which we have previously investigated.[37] These systems belong to the class of RAHBs. The rest of the systems are shown in Chart 1B. A complete listing of the systems is also provided as Supporting Information. Limited auxiliary studies were also done on benzoylacetone (**BA**) and hydrogen oxalate (**HO**) (Chart 1B).

Results and Discussion

Notation. QTAIM properties at both the (3, −1) O−H bond critical points (BCPs) and the O···H hydrogen bond critical points (HBCPs) will be used in the different analyses to be carried out. Hence, parameters at BCPs and HBCPs will be identified by subscripts b and hb, respectively.

Hydrogen Bridge Distances: *D*(O···H), *D*(O−H), and *D*(O···O). Because no BCP is observed for the O−O interactions, the dependence of QTAIM parameters on *D*(O···O) must use parameters obtained at HBCPs and/or BCPs. This is justified because changes in O−H, O···H, and O···O distances are expected to correlate[45,46] as the nature of the HB (which varies as a function of its electrostatic, dispersion, charge transfer, and covalent contributions[47]) changes. The expected correlation is

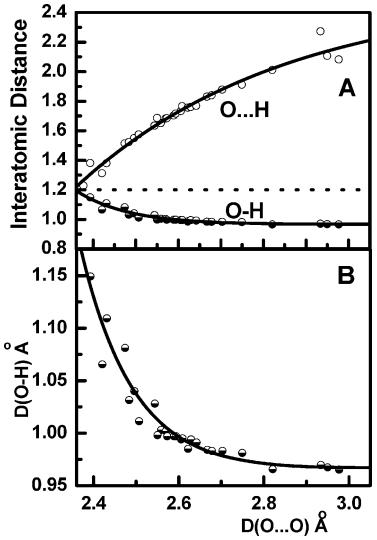

Figure 1. (A) Dependence of D(O−H) and D(O···H) on D(O···O). (B) Dependence of D(O−H) on D(O···O) showing the pronounced elongation of the O−H bond when D(O···O) < 2.55 Å in agreement with the PCC[8] classification. Distances are from B3LYP/6-311++G-(d,p) calculations. An auxiliary analysis also showed the correlation of D(O−H) with D(O···H) to be exponential, in agreement with the exponential behavior reported by several groups from use of experimental[45] and theoretical data.[21c] Solid curves are the best nonlinear fits for the data points.

confirmed as displayed in Figure 1. As can be seen in the inner part of Figure 1A, D(O···H) ≈ D(O−H) ≈ 1.2 Å at D(O···O) ≈ 2.37 Å, which can also be confirmed from the entries in Table 1 for D(O···H) and D(O−H) of system **1.** The AIM data for selected systems (data on all systems are provided as Supporting Information) in Table 2 show that $\nabla^2\rho_{hb} < 0$ and $|V_{hb}|/G_{hb} > 2$ for system **1**. Hence, the HB for this system is in the SS regime as reported previously.[23e]

The inner part of Figure 1B clearly shows that very significant elongation of the O−H bond occurs below D(O···O) ≈ 2.55 Å. Hence, the data are very consistent with both the PCC-[8] and the GC-based GBFG[7] classifications.

Electron Density. Figure 2 shows the dependence of ρ_b and ρ_{hb} on D(O···O) from which one can deduce $\rho_b \approx \rho_{hb} \approx 0.18$ ea_0^{-3} when D(O···O) ≈ 2.37 Å. At long D(O···O) values, ρ_{hb} should be zero, and ρ_b can be estimated to be ∼0.36 ea_0^{-3}. Hence, overall ρ_b (ρ_{hb}) decreases (increases) by ∼0.18 ea_0^{-3} when the O−O contraction reaches the SS limit (at D(O···O) ≈ 2.37 Å; see Figure 2 for details). What is almost remarkable about Figure 2 is the symmetrical nature of the curves with respect to a horizontal line at a ρ value of ∼0.18 ea_0^{-3}, whereas such symmetry is not evident in Figure 1A with respect to a horizontal line at D(O−H) ≈ D(O···H) ≈ 1.2 Å. This means that even though there is an almost 1:1 correspondence in the loss versus gain of electron density at the, respectively, BCPs and HBCPs, there is no such 1:1 correspondence in the elongation versus contraction of, respectively, the O−H bond and O···H HB. It is of interest to note here also that significant elongation of the O−H bond (Figure 1B) occurs below D(O···O) ≈ 2.55 Å. The D(O···O) distances of 2.5 and 2.39−2.40 Å are key demarcation points for both the GC[7] and the PCC[8] classifications (vide supra). The fact that the more precipitous decrease (increase) in ρ_b (ρ_{hb}) and the more pronounced elongation of the O−H bond starts to be more pronounced at D(O···O) ≈ 2.55 Å may thus have some relevance to both the PCC[8] and the GC (GBFG) classifications.[7] However, despite the fact that the inner parts of Figures 1 and 2 are very consistent with both the PCC-[8] and the GC-based GBFG[7] classifications, a definitive elucidation of the physical bases of the underlying process that led to these results cannot be made here until further analysis of other AIM parameters is carried out.

TABLE 1: Comparison of Results from B3LYP and MP2 Calculations and IMHB Energies and HB Strengths (HBSs) of Selected Systems

	B3LYP/6-311++G(d,p)[a]			MP2/6-311++G(d,p)[a]				
MS[b]	O···O	O···H	O−H	O···O	O···H	O−H	$-E_{HB,A}$[c]	HBS[d]
1	2.377	1.2279	1.1493	2.364	1.1851	1.179	30	S
4	2.393	1.3808	1.0655	2.3887	1.3764	1.0573	27.9	S
2	2.4206	1.3122	1.1093	2.407	1.303	1.104	24.9	S
3	2.4311	1.3799	1.0811	2.4183	1.3604	1.0812	23.7	S
IIb	2.474	1.514	1.04	2.436	1.441	1.052	22	S
HO	2.4897	1.7119	0.9999	*e*	*e*	*e*	17.4	M
IIIb	2.496	1.55	1.028	2.492	1.539	1.0196	17.2	S
BA[f]	2.5069	1.5751	1.0114	2.5414	1.6216	0.9991	16.1[f]	S
Ibc	2.544	1.634	1.003	2.549	1.633	0.9969	13.5	M
I	2.589	1.703	0.997	2.584	1.686	0.9927	11.6	M
IIc	2.678	1.839	0.983	2.676	1.8228	0.979	9.4	M
IIac	2.703	1.878	0.981	*e*	*e*	*e*	8.4	W
6	2.7494	1.9121	0.9655	2.7499	1.9029	0.9628	5.63	W

[a] Distances are given in angstroms. [b] Molecular systems are as given in Chart 1. [c] IMHB energies, $E_{HB,A}$, are in kcal/mol, and all, other than those for **1**−**4** and **6**, were taken from ref 37. $E_{HB,A}$'s for **1**−**4** and **6** were estimated using a statistical model for estimating IMHB energies that we previously reported ($E_{HB,A} = -8.426 \times 10^5 \exp(-4.333\ D(O\cdots O))$, with D(O···O) obtained at the MP2/6-311++G(d,p) level).[37] The reasonableness of the estimates was checked with literature reports when available. The estimates are, for example, in good agreement with those reported for **2**,[48] **4**,[49] and **BA**.[9] [d] HB strengths S, M, and W denote, respectively, strong, moderate, and weak. It should be noted that **BA** has been reported to have a very strong HBs. [e] **HO** and **IIac** were two of the few systems on which MP2/6-311++G(d,p) calculation was not done; they are included here for the purpose of consistency with Table 2. [f] The $E_{HB,A}$ entry for **BA** was taken from ref 9. Our estimate using the above statistical model and D(O···O) of 2.501 Å, which was the experimentally observed value,[9] is −16.6 kcal/mol. If the D(O···O) of 2.5069 Å obtained at the B3LYP/6-311++G(d,p) level is used, then the estimate is −16.1 kcal/mol. The MP2 D(O···O) entry of 2.5414 Å for **BA** is too long as reported in ref 9; hence, this value is inappropriate to be used in our statistical model.

Total Energy Density, H_{hb}. The magnitudes of V_{hb} and H_{hb} represent the capacity of the system to concentrate electrons at the HBCPs.[12] Figures 3A and 3B show the dependences of, respectively, H_{hb} and $|V_{hb}|/G_{hb}$ on D(O···O). Closer examination of the plot shows a negative-to-positive cross-over at D(O···O) ≈ 2.7 Å, where $G_{hb} \approx |V_{hb}|$ or $H_{hb} = 0$, which establishes the demarcation between the PCS and the CS interactions.[15] The plot of Figure 3B that shows $|V_{hb}|/G_{hb} = 1$ obtained at D(O···O) ≈ 2.69 Å supports this finding.[15] The plot also establishes the demarcation between the CS- and the SS-type interactions at which $|V_{hb}|/G_{hb} = 2$ is obtained at D(O···O) ≈ 2.38 Å.[15] From an earlier report, we have identified the D(O···H) distance at which $H_{hb} = 0$ to be 1.86 Å at the B3LYP/6-311G(d,p) level.[37,51] Similar analyses at the B3LYP/6-311++G(d,p) and MP2/6-311++G(d,p) levels have also been done, and a summary of the findings is included as part of Table 3.

On the basis of the H_{hb} plot, five systems having $H_{hb} > 0$ belong to the PCS class, for which the interactions are destabilizing because $G_{hb} > |V_{hb}|$; i.e., locally the pressure by the electrons (G_{hb}) is greater than the local pressure (V_{hb}) on the electrons.[15,51] Out of those with $H_{hb} < 0$, system **1** has $|V_{hb}|/G_{hb}$ (= 2.38) > 2 (and a negative Laplacian ($\nabla^2\rho_{hb} \approx -0.152$ ea_0^{-5}; Table 2) and thus belongs to the SS category. The HBs for the remainder—which includes both MHBs and SHBs—

TABLE 2: Selected QTAIM Topological Parameters for Selected Systems[a]

MS[a]	O···O[b]	O···H[b]	ρ_{hb}[b]	$\nabla^2\rho_{hb}$[b]	$-V_{hb}$[b]	G_{hb}[b]	$-H_{hb}$[b]	$\lvert V_{hb}\rvert/G_{hb}$	BD[b]	HBS[c]
1	2.377	1.2279	0.1619	−0.1518	0.236	0.099	0.137	2.38	0.85	S
4	2.393	1.3808	0.1111	0.0453	0.1412	0.0763	0.0649	1.85	0.58	S
2	2.4206	1.3122	0.1289	0.0404	0.1657	0.0879	0.0778	1.89	0.6	S
3	2.4311	1.3799	0.1105	0.105	0.1321	0.0792	0.0529	1.67	0.48	S
IIb	2.474	1.514	0.0781	0.1397	0.0845	0.0597	0.0248	1.42	0.32	S
HO[d]	2.4897	1.7119	0.0509	0.1413	0.0485	0.0419	0.0066	1.16	0.13	M
IIIb	2.496	1.55	0.0711	0.1436	0.0755	0.0557	0.0198	1.36	0.28	S
BA[e,f]	2.5005	1.5643	0.068	0.1538	0.0728	0.0556	0.0172	1.31	0.25	S
BA	2.5068	1.5751	0.0662	0.1525	0.0728	0.0542	0.0161	1.3	0.24	S
Ibc	2.544	1.634	0.0574	0.1456	0.058	0.0472	0.0108	1.23	0.19	M
I	2.589	1.703	0.0484	0.1341	0.046	0.0398	0.0062	1.16	0.13	M
IIc	2.678	1.839	0.0346	0.1127	0.029	0.0286	0.0004	1.02	0.01	M
IIac	2.703	1.878	0.0316	0.1056	0.0258	0.0261	−0.0003	0.99	−0.01	W
6	2.7494	1.9121	0.0259	0.1049	0.0216	0.0239	−0.0023	0.9	−0.09	W

[a] Molecular systems. All results are obtained at the B3LYP/6-311++G(d,p) level unless otherwise indicated. [b] Units are: for O···O and O···H distances in angstroms; for ρ_{hb} in ea_0^{-3}; for $\nabla^2\rho_{hb}$ in ea_0^{-5}; for V_{hb}, G_{hb}, and H_{hb} in hartrees per atomic unit volume; for BD ($= -H_{hb}/\rho_{hb}$) in au/ea_0^{-3}. [c] HB strengths S, M, and W denote, respectively, strong, moderate, and weak. [d] **HO** has been characterized not to be a LBHB even though its D(O···O) is <2.500 Å.[50] [e] Results are from B3LYP/6-311G(d,p) calculations. [f] **BA** has been characterized as a very strong HB bond on the basis of experimental and theoretical studies.[9] Additional discussion is given on both **HO** and **BA** in a later subsection, entitled the cases of BA and HO.

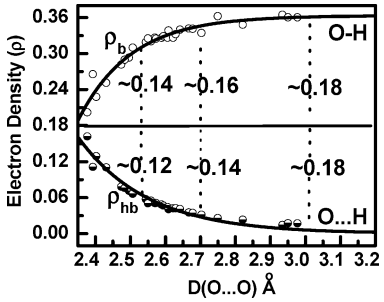

Figure 2. Dependence of the electron densities ρ_b and ρ_{hb} on D(O···O). As D(O···O) contracts from D(O···O) > 3 to ∼2.7 Å (a change in D(O···O), ΔD(O···O), of >0.3 Å), the net loss (gain) in ρ_b (ρ_{hb}) at the BCPs (HBCPs) are, respectively, 0.02 and 0.04 ea_0^{-3}. A further contraction of D(O···O) from 2.7 to about 2.55 Å (ΔD(O···O) = 0.15 Å) is accompanied by a net loss (gain) in ρ_b (ρ_{hb}) of only ∼0.02 ea_0^{-3}. However, in the range of 2.55−2.37 Å (ΔD(O···O) = 0.18 Å), the net loss and gain in ρ_b and ρ_{hb} are, respectively, 0.14 and 0.12 ea_0^{-3}, indicating that the net loss and gain for this last segment far outweigh those for the previous two. This figure is to be compared with Figure 1, and the data for both are in agreement with the PCC[8] and GC[7] classifications. Solid curves are the best nonlinear fits (R^2 = 0.946 for ρ_b and R^2 = 0.956 for ρ_{hb}) for the data points.

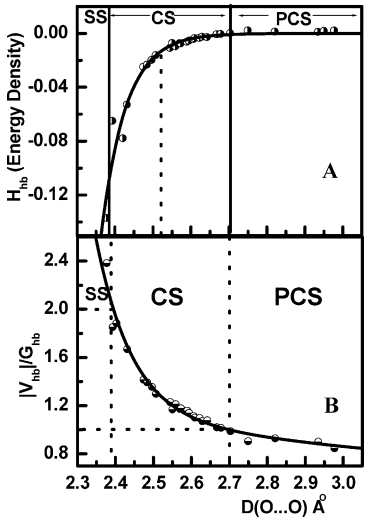

Figure 3. Dependence of (A) H_{hb} and (B) $|V_{hb}|/G_{hb}$ on D(O···O) showing the separation of the interatomic interactions into shared-shell (SS) (characterized by $H_{hb} < 0$ and $|V_{hb}|/G_{hb} > 2$), closed-shell (CS) (characterized by $H_{hb} < 0$ and $1 < |V_{hb}|/G_{hb} < 2$), and purely closed-shell (PCS) (characterized by $H_{hb} > 0$ and $|V_{hb}|/G_{hb} < 1$) interactions.[15] Solid curves are the best nonlinear fit for the data points. The dashed vertical line in part A is an internal border that roughly corresponds to the delimitation between strong and moderate HBs in accordance with the GC[7] and PCC[8] classifications.

belong to the CS type for which $H_{hb} < 0$ and thus have varying degrees of partial covalency because the accumulation of charge in the internuclear region is net stabilizing; i.e., $|V_{hb}| > G_{hb}$.[15−19,37] But, unlike the GC empirically based classification (Table 3), the CS classification does not distinguish between MHBs and SHBs. For example, in the $|V_{hb}|/G_{hb}$ plot (Figure 3B) a clear transition point from MHBs to SHBs is not observed. However, if one uses the GC (or PCC) demarcation border of D(O···O) ≈ 2.5−2.55 Å as indicated by the vertical line in Figure 3A, an interesting feature of the H_{hb} plot is the strong dependence on D(O···O) in the interior part of the figure (Figure 3A, left of the vertical dashed line). But, despite this interesting feature, the curve does not show a clear demarcation point.

Bond Degree Parameter, H_{hb}/ρ_{hb}. The ratio H_{hb}/ρ_{hb} has been rationalized as a bond or covalent degree parameter.[15] To see if this parameter would distinguish between MHBs and SHBs, the plots of H_{hb} and H_{hb}/ρ_{hb} versus D(O···O) are compared in Figure 4. However, the H_{hb}/ρ_{hb} plot does not seem to manifest any apparent distinctive feature. But, in the focused plot of Figure 4B, the data in the range of 2.5−2.7 can be modeled by a linear fit, while the data to the left of the vertical dashed line deviate from the linear plot, suggesting that the plots may be reminiscent of a "biphasic" behavior (with one phase representing MHBs and the other representing SHBs). This "biphasic" behavior, which would be consistent with the GC classification, is probed more closely in the next subsections.

Laplacian of the Electron Density, $\nabla^2\rho$. The dependence of $\nabla^2\rho$ on HB distances such as D(O···H) or D(F···H)[15] is routinely investigated in the literature. In addition to the dependence of $\nabla^2\rho_{hb}$ on D(O···H), we have also investigated the dependence of $\nabla^2\rho_{hb}$ on D(O···O), the first such study to our knowledge, for the systems investigated in the present work. (The plot is not shown here because a plot of the more intuitive function $L(r) = -\nabla^2\rho(r)$[27] is presented in the next subsection.) Two key features of such plots are the positions where (i) $\nabla^2\rho_{hb} = 0$ (denoted by d_{L0}) and (ii) the maximum in $\nabla^2\rho_{hb}$ ($\nabla^2\rho_{hb,max}$) (which we denote by $d(\nabla^2\rho_{hb,max})$) are obtained. On the basis of our analysis, entries for d_{L0} and $d(\nabla^2\rho_{hb,max})$ are included in Table 3 (in terms of both D(O···O) and D(O···H)).

Consistent with our earlier discussions, the internal border

TABLE 3: Compilation of Values of Various Parameters for PCS, CS, and SS Interaction Domains Including a Separation of the CS Domain into MHBs and SHBs[a]

AIM Classification	PCS	CS	SS	L_{hb}[b] ($\nabla^2\rho_{hb,max}$)
AIM criteria	$\lvert V_{hb}\rvert/G_{hb} < 1$ $H_{hb} > 0$; $\nabla^2\rho > 0$	$1 < \lvert V_{hb}\rvert/G_{hb} < 2$ $H_{hb} < 0$; $\nabla^2\rho > 0$	$\lvert V_{hb}\rvert/G_{hb} > 2$ $H_{hb} < 0$; $\nabla^2\rho < 0$	
internal borders[c]	$d_{H0} = 1.84$ (2.69) $H_{hb} = 0$	$d_{H0}-d_{L0}$	$d_{L0} = 1.3$ (2.38)[d] $\nabla^2\rho_{hb} = 0$	$d_{L,min}$
D(O···H) (Å)[e]	≥1.84	1.84−1.3	1.3 (1.3)	1.6 (1.54)
D(O···O) (Å)[e]	≥2.69	2.7−2.37	2.37 (2.38)	2.52 (2.5)
GBFG[f] D(O···O) (Å)	≥2.85−2.69	≥2.75−2.65 (M) 2.55−2.3 (S)		
EC (this work, on the basis of $-E_{HB,A}$)[g]	0 to ≤7	7 to 16 (M) ≥16 (S)	≥27.5	∼ 16[g]
$\lvert V_{hb}\rvert/G_{hb}$[h]	≤1	1−1.3 (M)1.3−2 (S)	≥2	∼1.3
$\lvert V_{hb}\rvert - 2G_{hb}$[h]	≥−17.5	−17.5 to −23 (M) −23 to 0 (S)	≥0	∼ −23
$-H_{hb}/\rho_{hb}$[h]	≤0	0−0.23 (M) 0.23−0.65 (S)	≥0.65	∼0.23
δ_{hb}(O,H)[i]	0−0.06	0.06−0.12 (M) 0.12−0.2 (S)	≥0.2	∼0.11−0.13

[a] Results are obtained at the B3LYP/6-311++G(d,p) level unless otherwise indicated. M and S denote, respectively, MHBs and SHBs. [b] Values are those obtained at the minimum (maximum) in the geometric dependence of L_{hb} ($\nabla^2\rho_{hb}$). [c] Values are D(O···H) and D(O···O) (in parentheses) distances. [d] d_{L0} is obtained at D(O···H) ≈ 1.3 Å at both the B3LYP/6-311++G(d,p) and the HF/6-311++G(d,p)//MP2/6-311++G(d,p) levels. This value is consistent with that reported (1.33 Å) previously from experimental densities.[19a] By comparison, for F−H···F−H systems, d_{L0} and d_{H0} were shown to be at D(F···H) distances of, respectively, 1.2 and 1.96 Å.[15] $\nabla^2\rho_{hb,max}$ was also shown to be at ∼1.35 Å but was not identified as an internal border between MHBs and SHBs.[15] [e] Ranges of D(O···H) and D(O···O) values for PCS, CS, and SS interaction domains except in the case of L_{hb}. Values in parentheses are MP2/6-311++G(d,p) results. [f] Values are delimitations for the GC classification.[5] [g] A refined energetics-based classification. Because the very strong HB system **BA** is reported to have a $E_{HB,A}$ value of −16.1 kcal/mol[9] (Table 1) and the $E_{HB,A}$ values of IMHBs may have errors of 1−1.5 kcal/mol,[37] the value at $d_{L,min}$ of −17.5 kcal/mol obtained from Figure 8 has been adjusted slightly to correspond to that of **BA**. [h] Ranges of values for PCS, CS, and SS interaction domains except in the case of L_{hb}. Units are: for $\lvert V_{hb}\rvert - 2G_{hb}$ in kcal/mol per atomic unit volume; for H_{hb}/ρ_{hb} in au/ea_0^{-3}. [i] DIs in pairs of electrons. Results are obtained at the HF/6-311++G(d,p)//MP2/6-311++G(d,p) level.

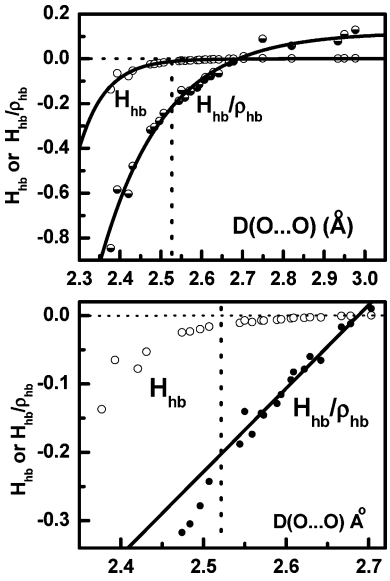

Figure 4. Plots of H_{hb} and H_{hb}/ρ_{hb} vs D(O···O). The figure compares the behavior of H_{hb} and H_{hb}/ρ_{hb} (top and bottom). Solid curves in the top panel are the best nonlinear fits for the data points. The dashed vertical lines in both figures are internal borders that roughly correspond to the delimitation between strong and moderate HBs in accordance with the GC[7] and PCC[8] classifications. In the focused bottom panel, the solid line is a linear fit of the data in the region to the right of the dashed vertical line.

d_{L0} is at D(O···O) ≈ 2.38 Å (Table 3). It is of interest to note that this d_{L0} value is apparently very close to the distance that is obtained when (i) $\rho_b \approx \rho_{hb}$ and (ii) D(O−H) ≈ D(O···H) (see Figures 1 and 2 for details). As indicated in Table 3, the D(O···O) value for $d(\nabla^2\rho_{hb,max})$ is ∼2.51 Å. Two very interesting conjectures can be made concerning this $d(\nabla^2\rho_{hb,max})$ value. First, the ∼2.51 Å value is very close to the 2.5 Å value of D(O···O) that is often implicated as the distance at which the onset of the pronounced elongation of the O−H bond sets in (in accordance with the PCC classification[8]). Second, the ranges $d_{L0}-d(\nabla^2\rho_{hb,max})$ (2.38−2.51 Å) and $d(\nabla^2\rho_{hb,max})-d_{H0}$ (2.51−2.69 Å) closely mesh, respectively, with the delimitations for strong and moderate HBs as advanced by the GBFG GC classification[7] (see Table 3 for details). We therefore propose $d(\nabla^2\rho_{hb,max})$ (∼2.51 Å) as an internal border that separates the regime of MHBs from that of SHBs. (In the SHB case, we do not make a distinction in this report between strong low barrier HBs (LBHBs) and short strong HBs (SSHBs)). Aside from the consistency of $d(\nabla^2\rho_{hb,max})$ (∼2.51 Å) with both the PCC[8] and the GC classifications,[7] what is proposed here is in fact that $d(\nabla^2\rho_{hb,max})$ should be regarded as a unique internal boundary (much like the two unique boundaries, d_{L0} and d_{H0}) that separates MHBs from SHBs. An important question should however be asked here. Are there underlying physical attributes that would make the newly proposed internal border ($d(\nabla^2\rho_{hb,max})$) a unique transition point that separates MHBs from SHBs? The next three subsections examine this fundamental issue from several vantage points.

Degrees of Charge Depletion. In general, if $\nabla^2\rho < 0$ at a given point, then charge is locally concentrated at that point, and if $\nabla^2\rho > 0$, then charge is locally depleted.[12] Across the CS region, $\nabla^2\rho > 0$ for all of the systems, and hence charge is locally depleted in all cases. To obtain more insight into the different degrees of charge depletion in the CS region, we will use the more intuitive function $L(r)$, i.e., $L(r) = -\nabla^2\rho(r)$,[27] whose dependence on D(O···O) is displayed in Figure 5. As the HB strength increases toward the SS limit, L_{hb} decreases until it reaches a minimum in L_{hb} ($L_{hb,min}$) at d(O···O) ≈ 2.51 Å. This means that the degree of charge depletion (DCD) increases and reaches a maximum at d(O···O) ≈ 2.51 Å. We shall denote this $L_{hb,min}$ distance (which corresponds to $\nabla^2\rho_{hb,max}$) by $d_{L,min}$ (= $d(\nabla^2\rho_{hb,max})$). Below $d_{L,min}$, L_{hb} increases with a strong dependence on D(O···O). Hence, the DCD decreases in

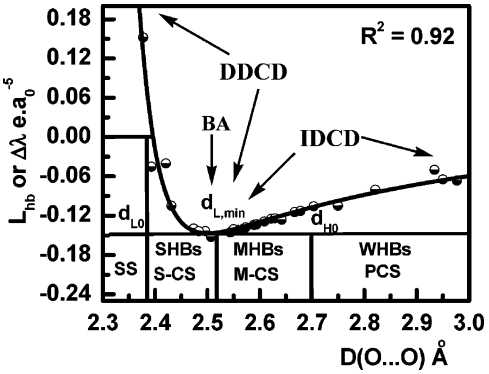

Figure 5. Characterization of the internal border for the transition from MHBs to SHBs from the dependence of $L_{hb} = \Delta\lambda\ (= |\lambda_1 + \lambda_2| - \lambda_3)$ on D(O···O). The figure models the competition between the perpendicular compressions (represented by $|\lambda_1 + \lambda_2|$) and the parallel expansion (represented by λ_3) of ρ at the HBCPs. $|\lambda_1 + \lambda_2|$ dominates when D(O···O) < 2.38 Å) (or, on the D(O···H) scale, at D(O···H) < 1.3 Å, plot not shown), and $|\lambda_1 + \lambda_2| > \lambda_3$ or, $\Delta\lambda > 0$. In contrast, λ_3 dominates when D(O···O) > 2.38 Å (or, on the D(O···H) scale, at D(O···H) > 1.3 Å, plot not shown), and $\Delta\lambda < 0$. The minimum in L_{hb} ($L_{hb,min} \approx -0.145\ ea_0^{-5}$ (at the B3LYP/6-311++G(d,p) level of theory)) is obtained at $d_{L,min}$ (∼2.52 Å). With O−O contraction, a region of increasing degree of charge depletion (IDCD) transitions to a region of decreasing degree of charge depletion (DDCD) at $d_{L,min}$. The data point for **BA** (Chart 1B) is just to the left of $d_{L,min}$. Both the MHBs and the WHBs fall in the IDCD region (D(O···O) > $d_{L,min}$), whereas SHBs fall in the DDCD region (D(O···O) < $d_{L,min}$). S−CS and M−CS denote, respectively, the SHB and MHB regions of CS. The internal borders d_{L0} and d_{H0} separate, respectively, SS from CS and CS from PCS. The solid line represents the best nonlinear fit by a sum of a power law and exponential function with a high degree of fidelity (R^2 = 0.92).

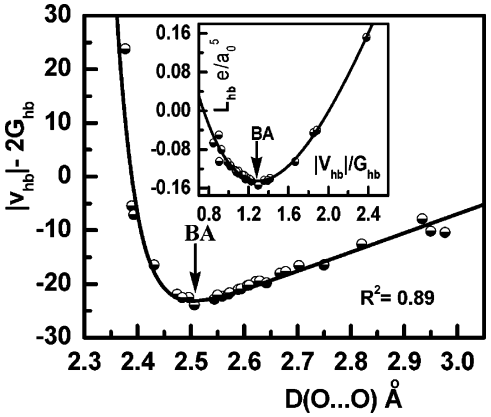

Figure 6. Dependence of the energy density difference $\Delta p = |V_{hb}| - 2G_{hb}$ (kcal/mol per atomic unit volume) on D(O···O), which shows a biphasic behavior. The figure models the mechanics of the interactions at the HBCPs, which can be viewed as a competition between the pressure on (V_{hb}) and by ($2G_{hb}$) the electrons. This figure is to be compared with Figure 5 because $\Delta\lambda \propto \Delta p$. With O−O contraction, Δp decreases (increases) in the IDCD (DDCD) region (cf. Figure 5). The trend in Δp behavior does not show any distinction between MHBs and WHBs. The inset shows the dependence of L_{hb} ($\Delta\lambda$) on the ratio $|V_{hb}|/G_{hb}$. The position of the minimum in L_{hb} occurs when $|V_{hb}|/G_{hb} \approx$ 1.3 (which corresponds to the minimum in the Δp plot that is obtained at D(O···O) ≈ 2.52 Å = $d_{L,min}$); $|V_{hb}|/G_{hb}$ has to be greater than ∼1.3 before the decrease in Δp (with O−O contraction) transitions to an increase in Δp at $d_{L,min}$. Arrows point to the data points for **BA**. The solid line represents the best nonlinear fit by a power law function (R^2 = 0.892). For the inset, the sum of an exponential and a linear function was used (R^2 = 0.982).

this range as D(O···O) approaches the SS limit. The plot, therefore, models a biphasic behavior in which a region of increasing DCD (representing MHBs and WHBs) transitions to a region of decreasing DCD (representing SHBs) at $d_{L,min}$.

Competition between Perpendicular Contractions and Parallel Expansion of ρ. According to AIM theory, the formation of a chemical bond and its associated interatomic surface are the result of a competition between the perpendicular contractions (characterized by the curvatures λ_1 and λ_2 (with $\lambda_1 \leq \lambda_2 < 0$)) of ρ (toward the bond path which leads to a concentration or compression of charge along this line) and the parallel expansion (characterized by the curvature λ_3 (with $\lambda_3 > 0$)) of ρ (away from the surface which leads to its separate concentration in each of the atomic basins).[12] Hence, the underlying phenomena at $d_{L,min}$ can be explained in terms of competition between perpendicular contractions and parallel expansion of ρ. Remembering that $\nabla^2\rho_{hb} = \sum\lambda_i$ ($i = 1-3$), if we now express L_{hb} as the difference between the curvatures, then $L_{hb} = -\nabla^2\rho_{hb} = \Delta\lambda = |\lambda_1 + \lambda_2| - \lambda_3$. We use $\Delta\lambda$ instead of L_{hb} for the discussion in this section to emphasize that L_{hb} is in essence a difference in the curvatures. Thus, the dependence of $\Delta\lambda$ on D(O···O) may be used to examine the competition between the perpendicular contractions and the parallel expansion using Figure 5 because $\Delta\lambda = L_{hb}$. Figure 5 manifests the biphasic behavior alluded to earlier, because in the range d_{L0}−2.51 Å as D(O···O) becomes shorter, $\Delta\lambda$ becomes increasingly positive with a strong dependence on distance (emblematic of exponential behavior), while in the range 2.51−d_{H0} Å the dependence of $\Delta\lambda$ on distance is only modest and is almost linear. The upward curvature at D(O···O) values <2.51 Å is a manifestation of the $|\lambda_1 + \lambda_2|$ term becoming, in relative terms, increasingly more and more significant until it eventually starts to dominate at d_{L0}. Thus, Figure 5 can be viewed as a way of modeling the competition between the perpendicular compressions (represented by the $|\lambda_1 + \lambda_2|$ term) and the parallel expansion (represented by the λ_3 term) of $\rho(r)$. Accordingly, $d_{L,min}$ represents the "onset" of the eventual dominance of the perpendicular compressions of ρ over the parallel expansion of ρ as D(O···O) becomes shorter. In other words, at $d_{L,min}$ the imbalance between the perpendicular compressions and the parallel expansion starts to shift in favor of the perpendicular compressions. The $|\lambda_1 + \lambda_2|$ term may be viewed as a manifestation of the increasingly covalent nature of the interactions because as D(O···O) → < d_{L0}, O···H → O−H. This, in turn, means that $d_{L,min}$ represents the transition to increasingly greater covalent contribution to the HB interactions as the interaction progresses to the SS limit at d_{L0}. This being the case, L_{hb} (or $\Delta\lambda$) should correlate with bond degree parameters—a matter to be discussed in later sections. In summary, $d_{L,min}$ is a unique transition point that separates the CS regime into two regions (Figure 5): S−CS (SHB region of CS) and M−CS (MHB region of CS).

Mechanical Characteristics of the Interactions. Because $\nabla^2\rho_{hb}$, which is a property of the charge density, is related to the local contributions to the energy (i.e., to the mechanics of the interactions) through the expression of the local virial theorem (eq 1),[12] it is easy to see that L_{hb} (= $-\nabla^2\rho_{hb}$) is proportional to $|V_{hb}| - 2G_{hb}$. $V(r)$ and $G(r)$ are dimensionally equivalent to pressure, being, respectively, the pressure exerted on and by the electrons.[15] In fact, the Laplacian itself (cf. eq 1), if multiplied by the constant $\hbar^2/4m$, may be viewed as a measure of pressure exerted on the electron density.[27] Denoting the energy density difference by $\Delta p = |V_{hb}| - 2G_{hb}$, then $\Delta\lambda \propto \Delta p$, and the dependence of Δp on D(O···O), shown in Figure 6, can be used to examine the competition between V_{hb} and $2G_{hb}$ and obtain further insight into the mechanics of the interactions.

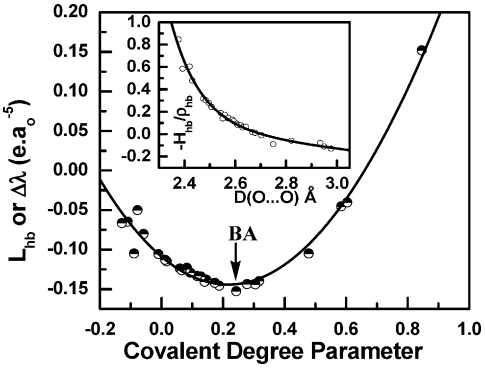

Figure 7. Correlation plot of L_{hb} ($= \Delta\lambda$) with the redefined bond degree (BD) parameter, BD $= -H_{hb}/\rho_{hb}$. An arrow points to the data point for **BA**. The inset shows the dependence of the redefined BD on D(O$\cdots$O). The solid lines represent the best nonlinear fit by the sum of an exponential and a linear function ($R^2 = 0.974$, main figure; $R^2 = 0.981$, inset).

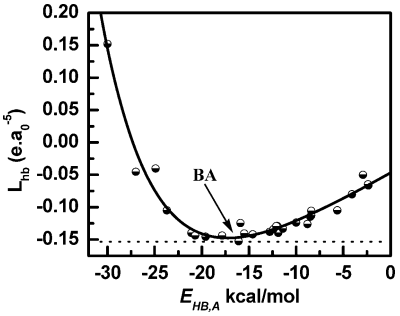

Figure 8. Correlation plot of L_{hb} ($= \Delta\lambda$) with the IMHB energy, $E_{HB,A}$. An arrow points to the data point for **BA**. The $E_{HB,A}$'s for some of the systems, obtained as the difference between the energies of the equilibrium geometries of the hydrogen-bonded and non-hydrogen-bonded forms at the MP2/6-311++G(d,p) level, were taken from our a previous report.[37] For the other systems, $E_{HB,A}$'s were obtained as noted in Table 1. The solid line represents the best nonlinear fit by the sum of an exponential and a linear function ($R^2 = 0.958$).

The plot of Figure 6A is clearly biphasic because Δp, with O−O contraction, decreases (increases) at distances $> d_{L,min}$ (at distances $< d_{L,min}$). In the range of $d_{L0}-d_{H0}$ in particular, $H_{hb} < 0$, and the potential energy density dominates over the kinetic energy density because $|V_{hb}|/G_{hb} > 1$ in this region. As can be discerned from Figure 3B, $|V_{hb}|/G_{hb} \approx 1.3$ at D(O$\cdots$O) ≈ 2.51 Å $= d_{L,min}$. This can also be confirmed from the plot of L_{hb} versus $|V_{hb}|/G_{hb}$ shown in the inset of Figure 6. Hence, $|V_{hb}|/G_{hb}$ has to be greater than ~1.3 before the decrease in Δp (with O−O contraction) transitions to an increase in Δp at $d_{L,min}$. Once this point is reached, the capacity to concentrate charge at the HBCP becomes increasingly significant as can be seen from the strong dependence on distance in the inner part of Figure 6 as opposed to the linear dependence at distances $> d_{L,min}$. This increasing capacity to concentrate charge at the HBCPs means a progressive increase in the covalent character of the HB. Hence, MHBs belong to $|V_{hb}|/G_{hb}$ values of 1−1.3, and SHBs to $|V_{hb}|/G_{hb}$ values of 1.3−2, with some SHBs having $|V_{hb}|/G_{hb} > 2$.

Correlation of L_{hb} with Other Parameters. In the preceding subsections, we have shown the utility of L_{hb} ($= -\nabla^2\rho_{hb}$) for the purposes of separating MHBs from SHBs. To illustrate further the importance of the $L(r)$ function, we will consider the correlation of L_{hb} with the bond degree (BD) parameter and the IMHB energy.

***L_{hb}*−Covalent Degree Parameter Correlation.** Espinosa et al.[15] defined BD as BD $= H_{hb}/\rho_{hb}$, as well as (i) a covalent degree (CD) parameter, CD $= H_{hb}/\rho_{hb} < 0$ for HBs in the CS interaction domain, and (ii) a softening degree (SD) parameter, SD $= H_{hb}/\rho_{hb} > 0$ for the PCS domain. However, BD did not provide any definitive transition point within the CS interaction regime as discussed in conjunction with Figure 4. Intuitively, it is more meaningful to associate bond degree parameters with positive values. Hence, much like the $L(r)$ function, we redefine the bond degree parameter as BD $= -H_{hb}/\rho_{hb}$, which yields positive values for CDs and negative values for SDs. Furthermore, the use of atomic units for H_{hb} and ρ_{hb} gives CD values between 0 and ~1 and SD values slightly below zero. A plot of CD and SD computed this way (using atomic units) versus D(O···O) is shown in the inset of Figure 7 while the main figure shows the excellent correlation of $\Delta\lambda$ ($= L_{hb}$) with CD and SD, the first of such study to our knowledge. From this figure, one can estimate the transition from MHBs to SHBs to occur at a value of CD ≈ 0.23. Beyond this point, as the covalent degree parameter increases, the DCD decreases. Furthermore, (i) the value of CD when $\Delta\lambda = 0$ can be estimated to be ~0.65, and (ii) when CD > 0.65, $\Delta\lambda$ ($= L_{hb}$) > 0, and the HB interaction is of the SS type. In summary, SHBs and MHBs have CD values in the ranges, respectively, ≥0.65−0.23 and 0.23−0, while WHBs have softening parameters SD < 0.

***L_{hb}*−IMHB Energy Correlation.** Figure 8 shows the correlation of L_{hb} with IMHB energies ($E_{HB,A}$'s), with the degree of correlation being excellent ($R^2 = 0.96$). This correlation, to our knowledge, is the first covering a wide spectrum of HB strengths. We should note, however, that the behavior observed here is at variance with the linear behavior reported previously,[5,52] and the Laplacian is not generally used to estimate HB energies. As is evident from the plot, two values of HB energies can be assigned from a given value of $\nabla^2\rho$. This finding makes it obvious why the Laplacian alone cannot provide unambiguous estimates for HB energies.

The minimum in the curve at $d_{L,min}$ corresponds to an $E_{HB,A}$ value of approximately −17.5 kcal/mol if B3LYP/6-311++G(d,p) L_{hb}'s are used. An auxiliary analysis using L_{hb} values determined at the HF/6-311++G(d,p)//MP2/6-311++G(d,p) level gave an excellent fit (with $R^2 = 0.997$) but still yielded −17.5 kcal/mol at $d_{L,min}$. This magnitude is reasonably close to the maximum (minimum) cut-off values for MHBs (SHBs) in accordance with some of the EC classifications (see table in the Introduction section). Recognizing that $E_{HB,A}$'s for IMHBs cannot be determined accurately,[37] it is very gratifying that the MHBs-to-SHBs transition identified here ($E_{HB,A} \approx -17.5$ kcal/mol) is in reasonable agreement with the EC-based classification of HB strengths.[6] With these values identified, a more uniform EC classification consistent with the GC classification can be reformulated using the internal borders identified from the QTAIM results. Such a juxtaposition is made in Table 3.

The Cases of BA and HO. As noted in Table 2 (and Table 1), **BA** has been characterized as a very strong HB system.[9] We have used **BA** here as a test case to support the validity of the identified internal border between SHBs and MHBs. Hence, data on **BA** were not included in any of the regression analyses; they were simply added to the plots in various figures. In most of the figures, the data point corresponding to **BA** has been labeled (Figures 5−8), and in all cases **BA** falls in the SHBs category although it is somewhat of a borderline case. The **HO** case is a rather interesting one. Its estimated $E_{HB,A}$ using our statistical model is on the order of −17.4 kcal/mol (see Table 1 for details). Its D(O$\cdots$O) of 2.4897 Å is less than the internal border $d_{L,min} \approx 2.51$ Å (Table 2). It ought to, therefore, be classified as an SHB system. However, its D(O$\cdots$H) of 1.7119 Å, which is greater than the internal border $d_{L,min} \approx 1.55$ Å,

TABLE 4: *D*(O···O), *D*(O···H), and *δ* (O,H) Values Obtained at the HF/6-311++G(d,p)//MP2/6-311++G(d,p) Level

MS[a]	*D*(O···O)(Å)	*D*(O···H)(Å)	*δ*(O,H)[b]
1	2.364	1.179	0.2396
4	2.3887	1.0573	0.1606
2	2.407	1.104	0.1945
3	2.4183	1.0812	0.1822
IIb	2.4362	1.052	0.1489
5	2.4501	1.0384	0.142
IIIb	2.4921	1.0196	0.1207
Ibc	2.5474	0.9969	0.0993
Ib	2.562	0.9959	0.0967
Ia	2.5602	0.9929	0.0936
Ic	2.5686	0.9947	0.0928
I	2.5839	0.9927	0.0901
IIIa	2.6026	0.9879	0.0829
IIa	2.6485	0.9836	0.0742
IIIc	2.6504	0.9809	0.0696
IIc	2.676	0.979	0.0661
6	2.7499	0.9638	0.0468
7	2.8244	0.9683	0.0443
8	2.9022	0.9628	0.0277
9	2.9521	0.9658	0.0380

[a] Molecular systems (cf. Chart 1). [b] In pairs of electrons.

would not be consistent with such a classification. Moreover, the transition from MHBs to SHBs, as shown here, is obtained when $|V_{hb}|/G_{hb} \approx 1.3$ and CD ≈ 0.23. As provided in Table 2, the $|V_{hb}|/G_{hb}$ and CD values for **HO**, respectively, ~1.156 and ~0.129 au/ea_0^{-3}, are below the transition values. **HO** should, therefore, belong to the MHB category. This conclusion is in agreement with a previous report in which **HO** was characterized not to be a LBHB system.[50] We note here that the case of **HO** should not be surprising, and it can serve as a reminder that O···O distances may not always be genuine indicators of the HB strength because the O atoms can be sometimes thrust together by steric, electronic, or other constraints.[37,53] Moreover, no single parameter can always effectively reflect all of the nuances of the HB interactions that arise from the interplay of various subtle modulations (which may in principle include one or more of π-electron conjugation superimposed on those of σ-electron delocalization, dipolar field/inductive and polarizability contributions, bond-length and bond-angle deformations, bond polarizations, or O···O repulsions). Hence, for questionable cases it is advisable to check several HB strength indicators before making a conclusion about the HB strength.

Electron Delocalization. Delocalization index calculations were done at the HF/6-311++G(d,p)//MP2/6-311++G(d,p) level on selected systems (as given in Table 4) representing all three classes of HB strengths (SHBs, MHBs, and WHBs). The DI calculations were also limited to atom pairs of the IMHB, i.e., to the O−H, O···H, and O···O cases denoted by, respectively, δ(O,H), δ_{hb}(O,H), and δ_{hb}(O,O). However, the discussion that follows will focus on δ_{hb}(O,H)'s only (for the sake of brevity), and a full report on these calculations is relegated to a future communication. δ_{hb}(O,H) values, all <0.25 (pairs of electrons), are tabulated in Table 4. The correlations between δ_{hb}(O,H) and the distance *D*(O···H), the electron density, ρ_{hb}, and the HB energy, $E_{HB,A}$, are presented in, respectively, Figures 9A, 9B, and 9C. Similarly, correlations of δ_{hb}(O,H) with other parameters are presented in Figures 10A−C.

***δ*$_{hb}$(O,H)−*D*(O···H) Correlation.** The dependence of δ_{hb}(O,H) on *D*(O···H) (Figure 9A) can be represented by an exponential model function with an excellent degree of correlation ($R^2 = 0.994$). Using the *D*(O···H) internal borders d_{L0} (1.3 Å), $d_{L,min}$ (1.55 Å), and d_{H0} (1.84 Å), Table 3, the respective

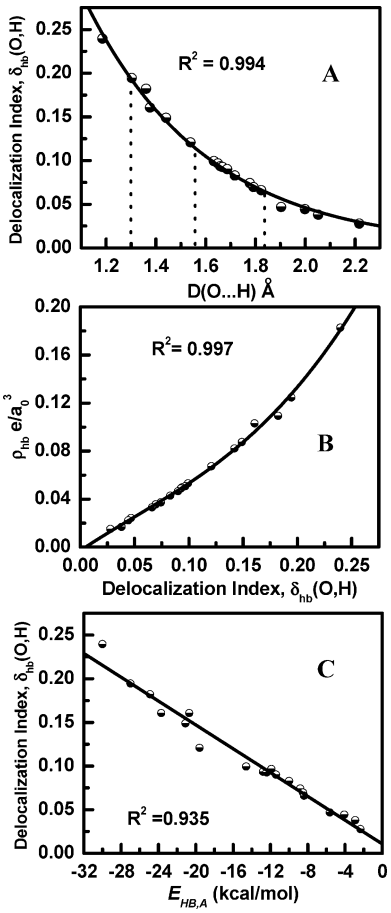

Figure 9. Correlation plots between δ_{hb}(O,H) and (A) *D*(O···H), (B) ρ_{hb}, and (C) the IMHB energy, $E_{HB,A}$. The solid lines represent the best fit to the data. For part A, the dependence is exponential. For part B, the best fit was obtained by a sum of polynomial (set a priori to degree of 2) and exponential model functions. For part C, the dependence is linear.

values of δ_{hb}(O,H) at these borders can be estimated from the figure, the estimates being (in pairs of electrons): for SHBs $\gtrsim$0.19; for MHBs 0.19−0.08; and for WHBs <0.06. The results indicate that there is a significant degree of electron delocalization even in the cases of the PCS interactions. However, because the DI calculation at the HF level does not have Coulomb correlation[54] and accounts only for the Fermi correlation,[35,55] the values should probably be somewhat lower at correlated levels of theory. Moreover, because the DIs were developed on the basis of the Fermi hole density[35,55] as a consequence of the Pauli exclusion principle, the results ought not be interpreted in terms of "partial covalency" in the PCS region. However, partial covalency has been predicted for the CS interactions.[15] But, the fact that considerable electron pairing is obtained even for the PCS interactions indicates that the δ_{hb}(O,H) values for the CS (and SS) interactions may not be interpreted as the sole consequence of covalency. This observation is consistent with the argument that DIs should be understood, in the strictest sense, as pair-density indices and should not always be viewed as bond indices.[30]

***ρ*$_{hb}$−*δ*$_{hb}$(O,H) Correlation.** Figure 9B displays the dependence of ρ_{hb} on δ_{hb}(O,H). The choice of model function for the dependence, an increase in ρ_{hb} as δ_{hb}(O,H) increases, was not however easy. Nonetheless, the best fit ($R^2 = 0.997$) was obtained by a sum of power and exponential law model functions, but the power law had to be set a priori to a polynomial of degree 2. Using the δ_{hb}(O,H) values that

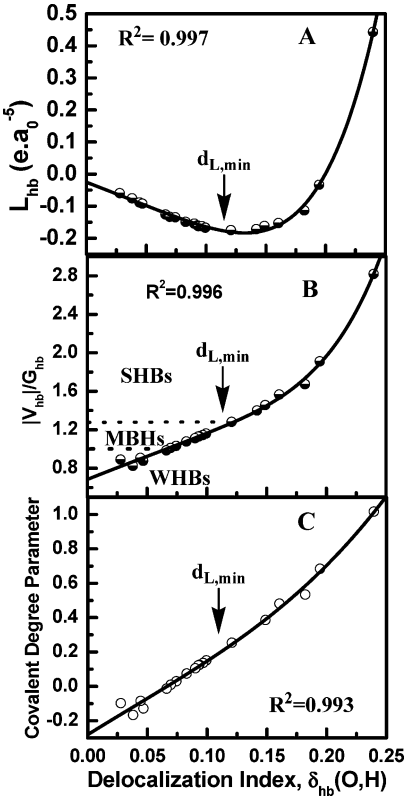

Figure 10. Correlation plots of δ_{hb}(O,H) with (A) L_{hb} (= $\Delta\lambda$), (B) $|V_{hb}|/G_{hb}$, and (C) the bond degree parameter (BD = $-H_{hb}/\rho_{hb}$). The solid lines represent the best fit for the data by the sum of an exponential and a power law function, in all cases with a high degree of fidelity. The approximate position where $d_{L,min}$ is obtained in the respective figures is indicated by an arrow.

correspond to the internal borders as identified from Figure 9A, the ρ_{hb} values at the internal borders d_{L0}, $d_{L,min}$, and d_{H0} can be estimated to be, respectively, 0.14, 0.06, and 0.03 ea_0^{-3}. However, the 0.14 ea_0^{-3} estimate appears to be somewhat low, most probably because the value obtained for d_{L0} ($\sim$1.3 Å) from the geometric (D(O$\cdots$H)) dependence of $\nabla^2\rho_{hb}$ is too low because the data in Figures 1 and 2 suggest that it should be on the order of 1.2 Å. In any case, the excellent degree of correlation between ρ_{hb} and δ_{hb}(O,H) suggests that δ_{hb}(O,H) may be estimated from experimental densities, or if reliable densities are available, without the need to carry out integrations over atomic basins.

***δ*hb(O,H)−IMHB Energy Correlation.** Figure 9C is a plot of δ_{hb}(O,H) versus IMHB energies ($E_{HB,A}$'s) that displays a linear correlation (R^2 = 0.935). As in the previous figure, this figure can also be used to estimate $E_{HB,A}$'s that correspond to the δ_{hb}(O,H) values at the internal borders. From such estimates, the ranges of the $E_{HB,A}$'s (in kcal/mol) that are obtained for the different HB strengths are: less than −16 for SHBs; −16 < $E_{HB,A}$ < −7 for MHBs; and between −7 and 0 for WHBs.

Correlations of *δ*hb(O,H) with Other Parameters. The correlations of δ_{hb}(O,H) with other parameters at HBCPs, L_{hb}, $|V_{hb}|/G_{hb}$, and BD (= $-H_{hb}/\rho_{hb}$), are presented in, respectively, Figures 10A, 10B, and 10C. A common feature that is manifested in all three cases is the biphasic nature of the plots (the BD case is somewhat less obvious) even though we have three different classes of HBs. The phase with linear or almost linear dependence of the three parameters on δ_{hb}(O,H) includes both the MHBs and the WHBs (which is consistent with the absence of clear evidence for a transition from WHBs to MHBs in the behavior of $\Delta\lambda$ and Δp (Figures 5 and 6)). This phase is followed by a very strong dependence on δ_{hb}(O,H) as seen particularly in Figures 10A and 10B. The biphasic nature manifested by $\nabla^2\rho(r)$ or the $L(r)$ function has been discussed in earlier sections. This biphasic behavior is not apparently unique to the Laplacian or the difference $\Delta p = |V_{hb}| - 2G_{hb}$. Fuster and Silvi have used the electron localization function to differentiate between weak, moderate, and strong HBs.[56] They found that the weak interaction was not a chemical interaction because the proton donor and acceptor molecules keep their individuality. Moderate HBs were found to be similar to the weak case, while the strong HB case corresponds to the formation of a new molecule by a chemical reaction. Hence, the similarity established in that work[56] may explain why no transition from WHBs to MHBs is observed in several of the figures alluded to above. In this regard, further work will be necessary to substantiate this presumption.

It has already been shown that the transition form MHBs to SHBs occurs at $d_{L,min}$ in the case of the Laplacian (Figure 5) and when $|V_{hb}|/G_{hb} \approx 1.3$ (Figure 6) and CD (= $-H_{hb}/\rho_{hb}$) $\approx$ 0.23 (Figure 7). The transition at these demarcation points, which transition from MHBs to SHBs, occurs at δ_{hb}(O,H) $\approx$ 0.125−0.13 as can be discerned from the plots in Figures 10A−C.

Summary and Conclusions

Unlike the simple monotonically decreasing exponential dependence on D(O$\cdots$O) and D(O$\cdots$H) observed for ρ_{hb}, the dependence of $\nabla^2\rho_{hb}$ is a "biphasic" curve with a single maximum, a transition point from an increase in $\nabla^2\rho_{hb}$ with distance to a decrease in $\nabla^2\rho_{hb}$. In the present investigation, the geometric dependence of the more intuitive function $L(r) = -\nabla^2\rho(r)$ as well as the function $|V(r)| - 2G(r)$, which is related to $L(r)$ through the local virial theorem, have been used to decode the chemical and physical bases of the biphasic behavior. Accordingly, the minima in the geometric dependence of L_{hb} and $|V_{hb}| - 2G_{hb}$ have been identified as the transition from MHBs to SHBs. For O−H$\cdots$O IMHBs, this transition is obtained, in a truly remarkable agreement with existing HB strength classifications, when the O$\cdots$O (O$\cdots$H) distance is $\sim$2.51 ($\sim$1.55) Å and when the ratio $|V_{hb}|/G_{hb}$) $\approx$ 1.3. The known SHB case of **BA** has been used to provide support for this finding. In rare cases for which the O$\cdots$O distance is not a genuine indicator of HB strength, the V_{hb}/G_{hb} ratio and/or other parameters should be considered to characterize the strength of the HBs. As to the physical basis of the transition, the behavior has been rationalized: (i) in terms of an increase (a decrease) in the DCD to the right (left) of the minimum at $d_{L,min}$ of the L_{hb}−D(O$\cdots$O) or L_{hb}−D(O$\cdots$H) curve as the O$\cdots$O or O$\cdots$H contraction occurs; (ii) in terms of the properties of ρ, as a competition between the perpendicular compressions (characterized by $|\lambda_1 + \lambda_2|$) and the parallel expansion (characterized by λ_3) of ρ at the HBCPs; or (iii) in terms the characteristics of the interactions that created the HBCPs, as a competition between the pressure on the electrons (V_{hb}) and the pressure by the electrons ($2G_{hb}$). Such analyses revealed the MHBs-to-SHBs transition (as O−O contraction occurs) corresponds to the point ($d_{L,min}$) of the onset of the dominance of (a) $|\lambda_1 + \lambda_2|$) over λ_3 and (b) V_{hb} over $2G_{hb}$.

The correlations between L_{hb} and other QTAIM parameters also have been explored in some detail. L_{hb} was found to correlate, with a very high degree of fidelity, with at least three such parameters: V_{hb}/G_{hb}, H_{hb}/ρ_{hb} (the so-called bond degree parameter), and the delocalization index, δ_{hb}(O,H). The specific values at $d_{L,min}$ are, respectively, 1.3, 0.23 au/ea_0^{-3}, and $\sim$0.11−

0.13 (pairs of electrons). L_{hb} was also found to correlate with the IMHB energy, $E_{HB,A}$, also with a very high degree of fidelity. These findings demonstrate the importance and utility of L_{hb} (or $\nabla^2\rho_{hb}$) for the study of HB interactions. For classification purposes, the ranges of values of some of the parameters can be summarized as follows: in terms of $|V_{hb}|/G_{hb}$ 1.3 to >2 for SHBs, 1−1.3 for MHBs, and <1 for WHBs; in terms of BD (CD/SD): ≥0.65−0.23 for SHBs, 0.23−0 for MHBs, and SD < 0 for WHBs; in terms of $E_{HB,A}$ (kcal/mol): less than −16 for SHBs; −16 to −7 for MHBs; and between −7 and 0 for WHBs. Thus, the study afforded the construction of a new refined energetics-based classification of IMHB strengths. Furthermore, the analyses can be extended to other intra- and intermolecular HB systems of different HB motifs (work in progress).

Acknowledgment. Partial support for this work was provided by the National Institutes of Health Minority Biomedical Research Support and Support of Continuous Research Excellence Programs (Grant No. S06-GM08247). This work has also benefited from the financial support for computer and software maintenance by a grant from the National Science Foundation Minority Research Centers of Excellence (Grant No. HRD-915407).

Supporting Information Available: Selected geometry data and Bader's QTAIM parameters (consisting of electron densities, potential and kinetic energy densities, and eigenvalues of the Hessian matrix of the electron density at O···H HB (3,−1) critical points). This material is available free of charge via the Internet at http://pubs.acs.org.

References and Notes

(1) Latimer, W. M.; Rodebush, W. H. *J. Am. Chem. Soc.* **1920**, *42*, 1419.

(2) (a) Joesten, M. D. *J. Chem. Educ.* **1982**, *59*, 362. This reference can be consulted for some of the books and reviews published prior to 1982. (b) Pimentel, G. C.; McClellan, A. L. *The Hydrogen Bond*; W.H. Freeman: San Francisco, CA, 1960 (Supplemental 1971). (c) Emsley, J. *Struct. Bonding* **1984**, *57*, 147. (d) Jeffrey, G. A.; Saenger W. *Hydrogen Bonding in Biological Structures*; Springer-Verlag: Berlin, 1991. (e) *The Hydrogen Bond: Recent Developments in Theory and Experiments*; Schuster, P., Zundel, G., Sandorfy, C., Eds.; North-Holland: Amsterdam, 1976. (f) *Modeling the Hydrogen Bond*; Smith, D. A., Ed.; ACS Symposium Series 569, American Chemical Society: Washington DC, 1994. (g) Scheiner, S. *Hydrogen Bonding*: *A Theoretical Perspective*; Oxford University Press: New York, 1997. (h) Jeffrey, G. A. *An Introduction to Hydrogen Bonding*; Oxford University Press: New York, 1997. (i) Desiraju, G. R.; Steiner, T. *The Weak Hydrogen Bond in Structural Chemistry and Biology*; Oxford University Press: New York, 1999. (j) Kollman, P. A.; Allen, L. C. *Chem. Rev.* **1972**, *72*, 283. (k) Desiraju, G. R. *Acc. Chem. Res.* **1976**, *29*, 441. (l) Bürgi, H.-B.; Dunitz, J. D. *Acc. Chem. Res.* **1983**, *16*, 153. (m) Gordon, M. S.; Jensen, J. H. *Acc. Chem. Res.* **1996**, *29*, 536. (n) Kirby, A. J. *Acc. Chem. Res*. **1997**, *30*, 290. (q) Hobza, P.; Sponer, J. *Chem. Rev.* **1999**, *99*, 3247.

(3) (a) For a minireview and references therein, see: Cleland, W. W.; Frey, P. A.; Gerlt, J. A. *J. Biol. Chem.* **1998**, *273*, 25529. (b) Kumar, G. A.; McAllister, M. A. *J. Am. Chem. Soc.* **1998**, *120*, 3159 and references therein.

(4) (a) Grabowski, S. J. *Annu. Rep. Prog. Chem., Sect. C: Phys. Chem.* **2006**, *102*, 131 and references therein. (b) Grabowski, S. J. *J. Phys. Org. Chem.* **2006**, *17*, 18 and references therein.

(5) Parthasarathi, R.; Subramanian, V.; Sathyamurthy, N. *J. Phys. Chem. A* **2006**, *110*, 3349.

(6) (a) Hibbert, F.; Emsley, J. J. *Adv. Phys. Org. Chem.* **1990**, *26*, 255. (b) Alkorta, I.; Elgeuro, J. *J. Phys. Chem. A* 1**999**, *103*, 272 and references therein.

(7) (a) Gilli, P.; Bertolasi, V.; Ferretti, V.; Gilli, G. *J. Am. Chem. Soc.* **1994**, *116*, 909. (b) Gilli, G.; Gilli, P. *J. Mol. Struct.* **2000**, *552*, 1. (b) Gilli, P.; Bertolasi, V.; Ferretti, V.; Gilli, G. *J. Am. Chem. Soc.* **2000**, *122*, 10405.

(8) (a) A classification of the strengths of O−H···O HBs on the basis of some physicochemical criteria (PCC) has been summarized this way:[8b] (i) the proton is confined to the potential well near one atom in the case of weak (normal) HBs; (ii) the zero-point vibrational energy (ZPVE) of the hydrogen (but not of deuterium) exceeds the proton transfer barrier for strong LBHBs; (iii) both the proton and the deuterium have sufficient ZPVE to shuttle between the two hydrogen-bonded atoms for very strong HBs. (b) Madsen, G. K. H.; Wilson, C.; Nymad, T. M.; McIntyre, G. J.; Larsen, F. K. *J. Phys. Chem. A* **1999**, *103*, 8684 and references therein.

(9) The ECHB model is supported by other works as well: (a) Schiøtt, B.; Iversen, B. B.; Madsen, G. K. H.; Bruice, T. C. *J. Am. Chem. Soc.* **1998**, *120*, 12117. (b) Madsen, G. K. H.; Iversen, B. B.; Larsen, F. K.; Kapon, M.; Reisner, G. M.; Herbstein, F. H. *J. Am. Chem. Soc.* **1998**, *120*, 10040.

(10) Desiraju, G. R. *Acc. Chem. Res.* **2002**, *35*, 565.

(11) Umeyama, H.; Morokuma, K. *J. Am. Chem. Soc.* **1977**, *99*, 1316 and references therein.

(12) Bader R. F. W. *Atoms in Molecules: A Quantum Theory*; Clarendon Press: Oxford, U. K., 1994.

(13) (a) Bader, R. F. W. *Phys. Rev. B* **1994**, *49*, 13348. (b) Bader, R. F. W.; Nguyen-Dang, T. T. *Adv. Quantum Chem.* **1981**, *14*, 63. (c) Bader, R. F. W.; Essen, H. *J. Chem. Phys.* **1984**, *80*, 1943. (d) Bader, R. F. W.; MacDougal, P. J.; Lau, C. D. H. *J. Am. Chem. Soc.* **1984**, *106*, 1594.

(14) (a) Cremer, D.; Kraka, E. *Angew. Chem., Int. Ed. Engl.* **1984**, *23*, 627. (b) Cremer, D.; Kraka, E. *Croat. Chem. Acta* **1984**, *57*, 1259. (c) Koch, W.; Frenking, G.; Gauss, J.; Cremer, D.; Collins, J. R. *J. Am. Chem. Soc.* **1987**, *109*, 5917.

(15) Espinosa, E.; Alkorta, I.; Elguero, J.; Molins, E. *J. Chem. Phys.* **2002**, *117*, 5529.

(16) (a) Bader, R. F. W. *J. Phys. Chem. A* **1998**, *102*, 7314. (b) Jenkins, S.; Morrison, I. J. *Chem. Phys. Lett.* **2000**, *317*, 97.

(17) Arnold, W. D.; Oldfield, E. *J. Am. Chem. Soc.* **2000**, *122*, 12835.

(18) Popelier, P. L. A. *J. Phys. Chem.* **1995**, *99*, 9747.

(19) (a) Espinosa, E.; Lecomte, C.; Molins, E. *Chem. Phys. Lett.* **1998**, *285*, 170. (b) Espinosa, E.; Lecomte, C.; Molins, E. *Chem. Phys. Lett.* **1999**, *300*, 745. (c) Espinosa, E.; Souhassou, M.; Lachekar, H.; Lecomte, C. *Acta Crystallogr., Sect. B* **1999**, *55*, 563.

(20) (a) Knop, O.; Rankin, K. N.; Boyd, R. J. *J. Phys. Chem A* **2001**, *105*, 6552. (b) Knop, O.; Rankin, K. N.; Boyd, R. J. *J. Phys. Chem A* **2003**, *107*, 272.

(21) (a) Ziolkowski, M.; Grabowski, S. J.; Leszczynski, J. *J. Phys. Chem. A* **2006**, *110*, 6514. (b) Grabowski, S. J.; Dubis, A. T.; Martynowski, D.; Glowka, M.; Palosiak, M.; Leszczynski, J. *J. Phys. Chem. A* **2004**, *108*, 5815. (c) Gora, R. W.; Grabowski, S. J.; Leszczynski, J. *J. Phys. Chem. A* **2005**, *109*, 6397.

(22) Mallinson, P. R.; Smith, G. T.; Wilson, C. C.; Grech, E.; Wozniak, K. *J. Am. Chem. Soc.* **2003**, *1125*, 4259.

(23) (a) Alkorta, I.; Elguero, J. *J. Phys. Chem. A* **1999**, *103*, 272. (b) Rosaz, I.; Alkorta, I.; Elguero, J. *J. Phys. Chem. A* **2001**, *105*, 10462. (c) Parthasarathi, R.; Subramanian, V.; Sathyamurthy, N. *J. Phys. Chem. A* **2005**, *119*, 843. (d) Sanz, P.; Mo, O.; Yanez, M.; Elguero, J. *J. Phys. Chem. A* **2007**, *111*, 3585. (e) Pakiari, A. H.; Eskandari, K. *J. Mol. Struct.* **2006**, *759*, 51.

(24) (a) Green, M. E. *J. Phys. Chem. A* **2002**, *106*, 11221. (b) Klein, R. A. *J. Comput. Chem.* **2002**, *23*, 585.

(25) (a) Galvez, O.; Gómez, P. C.; Pacios, L. F. *J. Chem. Phys.* **2003**, *118*, 4878. (b) Galvez, O.; Gómez, P. C.; Pacios, L. F. *Chem. Phys. Lett.* **2001**, *337*, 263.

(26) Gabanes, O.; Gómez, P. C.; Pacios, L. F. *J. Chem. Phys.* **2001**, *115*, 11166.

(27) Popelier, P. L. A. *Atoms in Molecules: An Introduction*; Prentice Hall: London, 2000.

(28) (a) Grabowski, S. J. *J. Phys. Chem. A* **2001**, *105*, 10739. (b) Grabowski, S. J. *Chem. Phys. Lett.* **2001**, *338*, 361. (c) Grabowski, S. J. *J. Mol. Struct.* **2001**, *562*, 137.

(29) Grabowski, S. J.; Sokalski, W. A.; Dyguda, E.; Leszczynski, J. *J. Phys. Chem. B* **2006**, *110*, 6444.

(30) Matta, C. F.; Hernandez-Trujillo, J. *J. Phys. Chem. A* **2003**, *107*, 7496.

(31) Matta, C. F.; Hernandez-Trujillo, J.; Bader, R. F. W. *J. Phys. Chem. A* **2002**, *106*, 7369.

(32) Poater, J.; Duran, M.; Sola, M.; Silvi, B. *Chem. Rev.* **2005**, *105*, 3911.

(33) (a) Fulton, R. L.; Perhacs, P. *J. Phys. Chem. A* **1998**, *102*, 9001. (b) Fulton, R. L. *J. Phys. Chem. A* **2006**, *110*, 12191. (c) Matta, C. F.; Castillo, N.; Boyd, R. J. *J. Phys. Chem B* **2006**, *110*, 563. (d) Tsirelson, V. G.; bartashevich, E. V.; Stash, A. I.; Potemkin, V. A. *Acta Crystallogr., Sect. B* **2007**, *63*, 142. (e) Poater, J.; Sola, M.; Duran, M.; Simon, S.; Fradera, X. *Theor Chem. Acc.* **2002**, *107*, 362. (f) Matito, E.; Poater, J.; Sola, M.; Duran, M.; Simon, S.; Salvador, P. *J. Phys. Chem. A* **2005**, *109*, 9904. (g) Poater, J.; Sola, M.; Duran, M.; Fradera, X. *J. Phys. Chem. A* **2001**, *105*, 2052. (h) Fradera, X.; Sola, M. *J. Comput. Chem.* **2003**, *25*, 439. (i) Feixas, F.; Matito, E.; Poater, J.; Sola, M. *J. Phys. Chem. A* **2007**, *111*, 4513. (j) Zhurova, E. A.; Matta, C. F.; Wu, N.; Zhurov, V. V.; Pinkerton, A. A. *J.*

Am. Chem. Soc. **2006**, *128*, 8849. (k) Wang, Y.-G.; Wiberg, K. B.; Werstiuk, N. H. *J. Phys. Chem. A* **2007**, *111*, 3592.

(34) Bader, R. F. W; Streitwieser, A.; Neuhaus, A.; Laidig, K. E.; Speers, P. *J. Am. Chem. Soc.* **1996**, *118*, 4959.

(35) Fradera, X.; Austen, M. A.; Bader, R. F. W. *J. Phys. Chem. A* **1999**, *103*, 304.

(36) Bader, R. F. W. *J. Phys. Chem. A* **1998**, *102*, 7314.

(37) Musin, R. N.; Mariam, Y. H. *J. Phys. Org. Chem.* **2006**, 19, 425.

(38) (a) Becke, A. D. *J. Chem. Phys.* **1993**, *98*, 5648. (b) Becke, A. D. *J. Chem. Phys.* **1992**, *96*, 2155. (c) Becke, A. D. *J. Chem. Phys.* **1992**, *97*, 9173. (d) Hehre, W. J.; Radom, L.; Schleyer, P. R.; Pople, J. A. *Ab Initio Molecular Orbital Theory*; Wiley: New York, 1986.

(39) A more detailed rationale along with some model chemistry studies has been provided in ref 37.

(40) Frisch, M. J.; Trucks, G. W.; Schlegel, H. B.; Scuseria, G. E.; Robb, M. A.; Cheeseman, J. R.; Montgomery, J. A., Jr.; Vreven, T.; Kudin, K. N.; Burant, J. C.; Millam, J. M.; Iyengar, S. S.; Tomasi, J.; Barone, V.; Mennucci, B.; Cossi, M.; Scalmani, G.; Rega, N.; Petersson, G. A.; Nakatsuji, H.; Hada, M.; Ehara, M.; Toyota, K.; Fukuda, R.; Hasegawa, J.; Ishida, M.; Nakajima, T.; Honda, Y.; Kitao, O.; Nakai, H.; Klene, M.; Li, X.; Knox, J. E.; Hratchian, H. P.; Cross, J. B.; Bakken, V.; Adamo, C.; Jaramillo, J.; Gomperts, R.; Stratmann, R. E.; Yazyev, O.; Austin, A. J.; Cammi, R.; Pomelli, C.; Ochterski, J. W.; Ayala, P. Y.; Morokuma, K.; Voth, G. A.; Salvador, P.; Dannenberg, J. J.; Zakrzewski, V. G.; Dapprich, S.; Daniels, A. D.; Strain, M. C.; Farkas, O.; Malick, D. K.; Rabuck, A. D.; Raghavachari, K.; Foresman, J. B.; Ortiz, J. V.; Cui, Q.; Baboul, A. G.; Clifford, S.; Cioslowski, J.; Stefanov, B. B.; Liu, G.; Liashenko, A.; Piskorz, P.; Komaromi, I.; Martin, R. L.; Fox, D. J.; Keith, T.; Al-Laham, M. A.; Peng, C. Y.; Nanayakkara, A.; Challacombe, M.; Gill, P. M. W.; Johnson, B.; Chen, W.; Wong, M. W.; Gonzalez, C.; Pople, J. A. *Gaussian 03*, revision B.4; Gaussian, Inc.: Wallingford, CT, 2004.

(41) *Spartan 04*; Wavefunction: Irvine, CA, 2004.

(42) Biegler-König, F.; Schönbohm, J.; Bayles, D. *J. Comput. Chem.* **2001**, *22*, 545.

(43) Wang, Y.-G.; Werstiuk, N. H. *J. Comput. Chem.* **2003**, *24*, 379.

(44) Kar, T.; Angyan, J. G.; Sannigrahi, A. B. *J. Phys. Chem. A* **2000**, *104*, 9953.

(45) (a) Nakamoto, K.; Margoshes, M.; Rundle, R. E. *J. Am. Chem. Soc.* **1955**, *77*, 6480. (b) Chiarri, G.; Ferraris, G. *Acta Crystallogr., Sect. B* **1982**, *38*, 2331. (c) Steiner, T.; Saenger, W. *Acta Crystallogr., Sect. B* **1994**, *50*, 348. (d) Bertolasi, V.; Gilli, P.; Ferretti, V.; Gilli, G. *Chem.—Eur. J.* **1996**, *2*, 925.

(46) (a) The different hydrogen-bonded systems were also shown to obey the same exponential dependence of D(O−H) on D(O···H) (plot not shown). This finding is consistent with the suggestion that the correlation curve can be regarded as a reaction path for proton transfer between two the oxygen atoms.[46b] (b) Steiner, T. *J. Phys. Chem. A* **1998**, *102*, 7041.

(47) Srinivasan, R.; Feenstra, J. S.; Park, S. T; Xu, S.; Zewail, A. H. *J. Am. Chem. Soc.* **2004**, *126*, 2266.

(48) (a) Tian, S. X.; Li, H.-B. *J. Phys. Chem. A* **2007**, *111*, 4404. (b) McAllister, M. A. *Can. J. Chem.* **1997**, *75*, 1195. (c) There also have been estimates in the range of 14−28 kcal/mol.[48d,e] (d) Woo, H.-K.; Wang, H.-B.; Wang, L.-S.; Lau, K.-C. *J. Phys. Chem. A* **2005**, *109*, 10633. (e) Bachi, R. D.; Dmitrenko, O.; Glukhovtsev, M. N. *J. Am. Chem. Soc.* **2001**, *123*, 7134.

(49) Madsen, G. K. H; Wilson, C.; Nymad, T. M.; McIntyre, G. J.; Larsen, F. K. *J. Phys. Chem. A* **1999**, *103*, 8684.

(50) Garcia-Viloca, M.; Gelabert, R.; Gonzalez-Lafont, A.; Moreno, M.; Lluch, J. M. *J. Am. Chem. Soc.* **1997**, *101*, 8727.

(51) (a) We acknowledge and thank the suggestion of a reviewer who suggested to us that some of the theoretical topological features such as ρ_{hb}, $\nabla^2\rho_{hb}$, and $\lambda_{i,hb}$ ($i = 1-3$) obtained for the weak HB systems may be compared to experimental values for O···H PCS interactions reported in ref 19c. (b) The same reviewer has also suggested to us that the D(O···H) distance of 1.86 Å at which $H_{hb} = 0$ obtained at the B3LYP/6−311G(d,p) level of theory may be compared to the 1.64 Å value estimated experimentally for intermolecular X−H···O systems (with X = C, N, O) as reported by Espinosa, et. al.[51c] We make note of these suggestions here for the benefit of readers who may be interested to pursue such comparisons. (c) Espinosa, E.; Molins, E. *J. Chem. Phys.* **2000**, *113*, 5686.

(52) (a) Knop, O.; Boyd, R. J.; Choi, S. C. *J. Am. Chem. Soc.* **1988**, *110*, 7299. (b) Boyd, R. J.; Choi, S. C. *Chem. Phys. Lett.* **1985**, *120*, 80. (c) Boyd, R. J.; Choi, S. C. *Chem. Phys. Lett.* **1986**, *129*, 62.

(53) Buemi, G.; Zuccarello, F. *Electron. J. Theor. Chem.* **1997**, *2*, 302.

(54) Bader, R. F. W.; Stephens, M. E. *J. Am. Chem. Soc.* **1975**, *97*, 7391.

(55) Love, I. *J. Phys. Chem. A* **2006**, *110*, 10507.

(56) Fuster, F.; Silvi, B. *Theor. Chem. Acc.* **2000**, *104*, 13.